Published in final edited form as:
Bone. 2012 January ; 50(1): 265–275. doi:10.1016/j.bone.2011.10.031.

Regulation of reactionary dentin formation by odontoblasts in response to polymicrobial invasion of dentin matrix

Nattida Charadram[a,b], **Ramin M Farahani**[a,b], **Derek Harty**[a], **Catherine Rathsam**[a], **Michael V Swain**[b], and **Neil Hunter**[a,b]

[a]Institute of Dental Research, Westmead Millennium Institute and Westmead Centre for Oral Health, Westmead, Sydney, New South Wales, Australia

[b]Faculty of Dentistry, University of Sydney, Sydney, New South Wales, Australia

Abstract

Odontoblast synthesis of dentin proceeds through discrete but overlapping phases characterized by formation of a patterned organic matrix followed by remodelling and active mineralization. Microbial invasion of dentin in caries triggers an adaptive response by odontoblasts, culminating in formation of a structurally altered reactionary dentin, marked by biochemical and architectonic modifications including diminished tubularity. Scanning electron microscopy of the collagen framework in reactionary dentin revealed a radically modified yet highly organized meshwork as indicated by fractal and lacunarity analyses. Immuno-gold labelling demonstrated increased density and regular spatial distribution of dentin sialoprotein (DSP) in reactionary dentin. DSP contributes putative hydroxyapatite nucleation sites on the collagen scaffold. To further dissect the formation of this altered dentin matrix, the associated enzymatic machinery was investigated. Analysis of extracted dentin matrix indicated increased activity of matrix metalloproteinase-2 (MMP-2) in the reactionary zone referenced to physiologic dentin. Likewise, gene expression analysis of micro-dissected odontoblast layer revealed up-regulation of *MMP-2*. Parallel up-regulation of tissue inhibitor of metalloproteinase-2 (*TIMP-2*) and membrane type 1- matrix metalloproteinase (*MT1-MMP*) was observed in response to caries. Next, modulation of odontoblastic dentinogenic enzyme repertoire was addressed. In the odontoblast layer expression of Toll-like receptors was markedly altered in response to bacterial invasion. In carious teeth *TLR-2* and the gene encoding the corresponding adaptor protein MyD88 were down-regulated whereas genes encoding TLR-4 and adaptor proteins TRAM and Mal/TIRAP were up-regulated. TLR-4 signalling mediated by binding of bacterial products has been linked to up-regulation of MMP-2. Further, increased expression of genes encoding components of the TGF-β signalling pathway, namely SMAD-2 and SMAD-4, may explain the increased synthesis of collagen by odontoblasts in caries. These findings indicate a radical adaptive response of odontoblasts to microbial invasion of dentin with resultant synthesis of modified mineralized matrix.

Corresponding authors: Dr.Nattida Charadram, DDS. Institute of Dental Research Level 2 Westmead Centre for Oral Health Westmead Hospital Sydney NSW, 2145 Phone(work) +61-2-9845-8767 Fax(work) +61-2-9845-7599 ncha1431@uni.sydney.edu.au . Nattida Charadram (ncha1431@uni.sydney.edu.au) Ramin M Farahani (rmos4386@uni.sydney.edu.au) Derek Harty (derek_harty@wmi.usyd.edu.au) Catherine Rathsam (catherine_rathsam@wmi.usyd.edu.au) Michael V Swain (mswain@mail.usyd.edu.au) Neil Hunter (neil_hunter@wmi.usyd.edu.au)

Conflict of interest: All the authors state that they have no conflicts of interest.

Supplemental data: There are supplemental data included with submission.

Keywords

Reactionary dentin; collagen network; DSP; matrix metalloproteinases; Toll-like receptors

Introduction

Dentin is a highly organized calcified matrix consisting of hydroxyapatite crystals overlayed on an underlying organic scaffold. The ontogeny of dentin closely reflects this structural arrangement; synthesis and secretion by odontoblasts of a collagenous network and associated non-collagenous proteins, so-called pre-dentin, is followed by subsequent remodelling and final mineralization to form mature dentin [1]. Likewise, during osteogenesis an initial unmineralized osteoid is synthesized which is later mineralized and converted to bone [2]. Implicit in this analogy is the deeper common phylogenetic origin of non-collagenous proteins (NCPs) of both tissues as a result of gene duplication events in the secretory calcium-binding phosphoprotein locus, the precursor site of most bone and dentin matrix proteins [3].

Optimal spatial configuration of mineralized tissues that is vital to many characteristic adaptive phenotypes, is foreshadowed by natural selection of a mineralized trait in the origin of vertebrates. Mineralized tissue has remained essentially unaffected by further divergence of life during evolution, unlike most other tissues [4]. Hence, structural abnormalities of mineralized tissues following functional aberrations of NCPs or associated proteins are manifested as a range of pathological phenotypes of dentin/bone [5]. While most pathological phenotypes carry significant morbidity, exceptions, where the resultant phenotype imparts remarkable adaptive capacity, have been reported [6].

Stimulation of odontoblasts following polymicrobial invasion of dentin in dental caries [7] induces an adaptive response characterized by altered functionality of odontoblasts and synthesis of modified dentinal matrix referred to as reactionary dentin, a relatively atubular dentin with altered biochemical properties [6, 8]. Radical structural rearrangement of dentin, for instance, diminished tubularity, ensues that this modified odontoblastic activity results in significant impedance of bacterial progression through dentin [6]. This is evident by the protracted nature of caries progression. Unravelling the cascade of molecular events preceding the functional shift of odontoblasts and the concomitant reactionary dentinogenesis will expand current knowledge of pathological mineralized tissue formation.

Anionic NCPs are high-affinity nucleators of calcium and hydroxyapatite, acting as anchorage sites which link the collagen network to mineral phase [9] and thus translate the spatial configuration of hard tissue dictated by collagen into the final mineral structure. Dentin sialophosphoprotein (DSPP), a major mineral phase-interactive acidic matrix protein of dentin secreted by odontoblasts, is essential for dentin formation [10, 11]. DSPP has also been found to be expressed in bone [12] and cementum [13]. Earlier work in our laboratory demonstrated that an important feature of odontoblastic activity during reactionary dentinogenesis is marked up-regulation of *DSPP* [6]. DSPP is secreted as a multidomain extracellular matrix protein of dentin sialoprotein (DSP) at the N terminus, followed by dentin glycoprotein (DGP) and dentin phosphoprotein (DPP) at the C terminus [14]. The activation process requires processing to release the active acidic moieties DSP and DPP that enhance mineralization by sequestering calcium ions [15]. Matrix metalloproteinases (MMPs) are implicated in this processing [14].

MMPs, a family of zinc-dependent endopeptidases, have been suggested to play an important role in the initiation of cartilage mineralization [16]. MMPs have the capacity to

degrade protein components in the extracellular matrix and are essential in the remodelling of connective tissue in both physiological and pathological conditions [17]. Matrix metalloproteinase-2 (MMP-2) is present in human osteoblasts [18, 19] and is abundantly expressed in odontoblasts and dentin [20, 21]. DSPP can be cleaved by MMP-2 releasing DSP from larger molecules [14]. It has been reported that MMP-2 has the capacity to regulate the bioavailability and bioactivity of transforming growth factor beta (TGF-β) [22]. MMP-2 is synthesized and released by human osteoblasts as an inactive pro-protein. Inactive pro-MMP-2 is subsequently activated by a process regulated by membrane type-1 matrix metalloproteinase (MT1-MMP) and tissue inhibitor of metalloproteinase-2 (TIMP-2) [23, 24].

The aim of the present study was to dissect the patho-physiological cascade culminating in the formation of reactionary dentin with particular focus on the following:

- Analysis of the micro-structure of reactionary dentin with reference to the collagenous framework and associated NCPs.
- The enzymatic machinery and associated regulatory proteins involved in reactionary dentinogenesis.
- Molecular basis for the functional shift of odontoblasts in caries-induced reactionary dentinogenesis.

To achieve these aims, the pattern of the collagenous scaffold of reactionary dentin was analysed and compared to physiologic dentin. Further, the anchorage pattern of DSP overlayed on collagen was assessed. Together with investigation of the associated enzymatic machinery responsible for synthesis of altered reactionary dentin, the data provides the first evidence for radical adaptive response of odontoblasts to synthesize a modified mineralized matrix in a non-stochastic context.

Materials and Methods

Materials and reagents

All chemicals were purchased from Sigma-Aldrich Inc. (MO) unless stated otherwise. The water used throughout the study was treated with diethyl pyrocarbonate (DEPC) to inhibit contaminating ribonucleases, as described elsewhere [6].

Tissues

Healthy non-carious and carious permanent molar teeth (30 carious and 15 healthy) were obtained from male and female patients aged 20 to 35 years who attended the dental clinics at the Westmead Centre for Oral Health, Westmead Hospital. The patients were otherwise healthy, without systemic conditions known to affect calcified tissues or immune responses. The selected carious teeth were restoration-free with caries originating as occlusal lesions with extensions ranging from one to two thirds of the depth of dentin. Healthy teeth were anatomically sound without any signs of attrition, abrasion or erosion leading to dentinal exposure or any associated pathologies affecting the pulp-dentin complex. The Ethics committee of Sydney West Area Health Service approved the study and the guidelines of the National Health and Medical Research Council of Australia were observed. All patients received written information on the research and signed a consent form.

Processing of the specimens

Immediately after extraction, the tooth was cleaned and a longitudinal groove prepared using diamond bur (NB Nova; Italy) with ample water cooling and without penetration into the dental pulp. Water coolant was treated with DEPC to inhibit contaminating ribonucleases.

Subsequently, the tooth was split into halves by mechanical leverage. The tooth half containing the pulp was fixed in 2% paraformaldehyde/5% sucrose in 0.02 M phosphate buffer, pH 7.4 (680 mOsm) for 2 h at 4°C. Photographs of fixed split tooth halves were taken under a dissecting stereomicroscope (Leica MZ8; Germany) to confirm proportional representation of the lesion. Also, to confirm that the dentinal lesion did not extend for more than 2/3 of the distance from the dentin-enamel junction to the nearest pulp border. For teeth that met this additional criterion the half not containing pulp was immediately used for sampling of dentin layers. The fixed tooth half containing pulp was demineralized in Morse's solution (22.5% formic acid and 10% sodium citrate) for 3 days at 4°C followed by dehydration through a graded series of ethanols, 15 minutes each at 4°C. A commercial glycol methacrylate embedding kit (ImmunoBed; Polysciences Inc., Warminster, PA) was used for embedding according to the manufacturer's protocol. Tissue blocks were stored tightly sealed at 4°C until the time of microtomy.

Fluorescence in situ hybridization (FISH)

Serial sections of 2 μm thickness of the tooth half that contained pulp were prepared on a Reichert Ultracut microtome (Leica; Germany). FISH was performed on the resin sections [25]. Briefly, sections were pre-treated with 0.2 M HCl for 10 min, washed in 18 MΩ water and treated with 1% Triton X-100 in 18 MΩ water. To assist penetration of FISH probe into bacteria, a digestion step was performed by using a proteinase cocktail (2 mg/ml proteinase K, 2 mg/ml lysozyme, and 1,000 U/ml mutanolysin in 10 mM phosphate buffer, pH 6.7) for 40 min at 37°C. Digestion was stopped using 2 mg/ml glycerine, sections washed in 50 mM Tris buffer pH 7.2, followed by washing in 18 MΩ water and left to air dry. A Gene Frame (ABgene; UK) was used to mount each sample for addition of 25 μl of hybridization buffer containing fluorescent probe at a concentration determined to be optimal for detection of bacteria. A universal bacterial probe, EUB 338 (5′- GCTGCCTCCCGTAGGAGT- 3′) labelled at the 5′ end with Alexa 594 (Invitrogen; Zymed Laboratories) was used. The sections were incubated overnight with 25% formamide stringency at 46°C using a Hybaid OmniSlide system (Hybaid) and washed in washing buffer using a Hybaid wash module. The sections were washed in cold 18 MΩ water and allowed to dry. The slides were coverslipped using ProLong Gold antifade reagent (Molecular Probes). The sections were visualized using an Olympus BX60 fluorescence microscope connected to a Leica DFC500 camera.

Fluorescence immunohistochemistry

Serial 2 μm sections were used for immunohistochemistry. For antigen retrieval, sections were incubated in 1 mM EDTA, pH 8 at 100°C for 30 minutes in a microwave oven, then sections were cooled to room temperature and washed in PBS for 5 min. Sections were blocked with 10% goat serum/PBS for 3 h followed by incubation overnight with primary antibody diluted in 10% fetal calf serum/PBS at 4°C. Primary antibodies included: mouse monoclonal MMP-2 (dilution 1/200; Invitrogen, Zymed Laboratories), rabbit monoclonal MT1-MMP (dilution 1/200; Invitrogen, Zymed Laboratories) and mouse monoclonal Endo 180 (dilution 1/200; Santa Cruz Biotechnology, Santa Cruz, CA). Negative control sections were also incubated overnight with isotype control antibody. After washing in PBS (3×10 min), sections were incubated with fluorochrome-conjugated secondary antibody diluted in 10% fetal calf serum/PBS at room temperature for 2 h. The secondary antibodies were goat anti-mouse IgG Alexa-594 (dilution 1/500; Invitrogen, Zymed Laboratories) or goat anti-rabbit IgG Alexa-488 (dilution 1/500; Invitrogen, Zymed Laboratories). The sections were then washed in PBS and mounted onto glass slides using ProLong Gold antifade reagent with DAPI (Invitrogen, Molecular Probes; Eugene, OR). The sections were viewed using an Olympus BX60 fluorescence microscope and images captured using a Leica DFC500 camera.

Dentinal structure investigated under FEI-SEM

Longitudinal- (n=6) and cross- (n=3) sections of dentin fragments in the area of reactionary dentin were prepared. Samples used for dentinal structure analysis (3 longitudinal- and 3 cross-sections) were demineralized in 10% citric acid for 2 min at room temperature. After rinsing with PBS, samples were incubated in 1 mg/mL TPCK-treated Trypsin (Sigma-Aldrich; St Louis, MO, USA; the inhibitor L-1-Tosylamide-2 phenylethyl chloromethyl ketone (TPCK) inhibits contaminating chymotrypsin, ensuring specificity of cleavage by trypsin) in 0.2 M NH_4HCO_3 at 37°C for 48 h and rinsed with PBS as it has been reported previously that trypsin digestion of dentin samples provides better visualisation of the diameter of collagen fibrils and also of the interfibrillar space [26]. Samples were immediately fixed in 2.5% glutaraldehyde in 0.1 M cacodylate buffer at pH 7.2 for 4 h and rinsed with 0.1 M cacodylate buffer at pH 7.2 for 1 h. After dehydration in a graded ethanol series (30%, 50%, 70%, 90%, 95% and 3 changes of 100%), samples were dried using hexamethyl disilazane (Sigma-Aldrich; St Louis, MO, USA) and mounted on stubs using a conductive tape and coated with gold/palladium (Emitech K550x; UK).Observations were performed using high resolution FEI-SEM (Zeiss ultra Plus; Oberkochen, Germany). Images were obtained using secondary electron detector at 10.00 kV.

For immuno-gold labelling, samples (n=3) from longitudinal-sections were fixed in 4% paraformaldehyde solution at 4°C for 12 h, then rinsed with PBS before demineralization. After incubation with 1 mg/mL TPCK-treated trypsin in 0.2 M NH_4HCO_3 for 24 h to provide optimal visualisation of gold particles on collagen fibrils, samples were immersed in 0.05 M TRIS HCL buffer solution (TBS) at pH 7.6 with 0.15 M NaCl and 0.1% bovine serum albumin, followed by 3 rinses for 10 min each. Samples were blocked in 10% goat serum in 0.05 M TBS at pH 7.6 for 30 min at room temperature, followed by incubation overnight at 4°C with primary antibody, mouse monoclonal DSP (dilution 1/100; Santa Cruz Biotechnology, Santa Cruz, CA), diluted in 0.05 M TBS, pH 7.6. Negative control sections were also incubated overnight with isotype control antibody. After rinsing with 0.05 M TBS at pH 7.6 and 0.02 M TBS at pH 8.2, samples were incubated with secondary antibody, goat anti-mouse IgG conjugated with 20nm colloidal gold particles (diluted 1:20; BBI international, UK) in 0.02 M TBS at pH 8.2 for 90 min at room temperature and rinsed with 0.02 M TBS, pH 8.2. Samples were fixed, dehydrated and dried as described above. Aftermounted on stubs using a conductive tape, samples were coated with carbon (Bal-Tec AG, Liechtenstein). Observations were performed under high resolution FEI-SEM (Zeiss ultra Plus; Oberkochen, Germany). Images were obtained using a combination of secondary electron and backscattered detectors at 10.00 kV.

Analysis of partially decalcified matrix structure

The altered structure of reactionary dentin (Rd) was analysed and compared to normal tubular dentin in the carious sample and to dentin in the healthy sample using scanning electron micrographs. The images were processed using ImageJ (version 1.41o; National Institutes of Health). For analysis, random regions of interest (ROI) [27] were selected and converted to binary images.

Distribution patterns and cross-sectional areas of dentinal tubules were analysed in nine random ROI from three samples in each group using the Surface Plot analysis tool (ImageJ version 1.41o; National Institutes of Health) which displays an intensity plot for foreground pixels of the ROI. Bars reflect the location and area of tubules in the ROI.

Circularity analysis of dentinal tubules was accomplished using Circularity Plugin (ImageJ version 1.41o; National Institutes of Health) on 30 random ROIs from three samples in each group.

The pattern of the collagen framework in each region was analysed by the lacunarity (λ) and fractal dimensions (D_F) technique using Fraclac Plugin (ImageJ version 1.41o; National Institutes of Health) (Supplementary Materials and Methods).

Analysis of distribution pattern and density of immuno-gold labelling

In order to analyse distribution pattern and density of labelling for DSP, regions of interest [27] were drawn using software (ImageJ version 1.41o; National Institutes of Health). The density of DSP in each region was analysed and expressed as percentage of the area occupied by DSP using the Measure analysis tool (ImageJ version 1.41o; National Institutes of Health).

The distribution pattern of immuno-gold labelling for DSP in each region was analysed using the Plot Profile analysis tool (ImageJ version 1.41o; National Institutes of Health).

Gene expression of odontoblasts in response to caries progression assessed using real-time qPCR

To investigate the change of expression of genes of interest in odontoblasts in response to caries progression, resin-embedded odontoblast layers from carious (n=6) and healthy (n=6) teeth were analysed by real-time qPCR. Micro-dissection of 12 consecutive 8 μm sections of the odontoblast layer adjacent to carious dentin and that of healthy teeth from a corresponding region were performed under a stereomicroscope (Leica Microsystems; Germany) (Fig. 7A).

Total RNA was extracted from the sections using RNeasy FFPE kit (Qiagen) according to the manufacturer's instruction. Total RNA yields from the extraction were quantified by A_{260} nm measurement (Nanodrop ND-1000; Thermo scientific) and quality of RNA in samples was investigated by Agilent RNA 6000 Pico chip (Agilent Technologies; Palo Alto, CA). SuperScript II reverse transcriptase (Invitrogen; Zymed Laboratory) was used for reverse transcription of extracted total RNA according to the manufacturer's protocol. Briefly, the reaction contained 4 μl of RNA, 1 μl of SuperScript II reverse transcriptase, 2 μl of random nanomer (Geneworks; Adelaide, South Australia) (final concentration of 10 μmol/L), 1 μl of deoxyribonucleotide triphosphate mix (10 mM each), 4 μl of 5X first-strand buffer, 2 μl of 0.1 M dithiothreitol, 1 μl of RNase inhibitor (40 units/reaction) and 5 μl of DEPC-treated water. The reverse transcription product, cDNA, was stored at −20°C until required for analysis.

Singleplex real-time qPCR was performed by using 2 μl of cDNA of the genes of interest on a Strategene Mx3005P Real-Time PCR system (Agilent Technologies; Palo Alto, CA) with the Platinum quantitative PCR Supermix-UDG (Invitrogen; Zymed Laboratories). Primers and Taqman probes were designed to span exon-exon junctions to prevent genomic DNA amplification for *MMP-2*, *TIMP-2*, *MT1-MMP*, *Endo180*, *TLR-2*,*-4*, *MyD88*, *TRAM*, *Mal/TIRAP*, *NF-κB*, *IκBα*, *SMAD-2*,*-4*, collagen type Iα1 *(COL1A1)* and collagen type Iα2 *(COL1A2)* (Supplementary Table 1). Each sample was run in triplicate in a 25 μl reaction volume on a 96-well PCR plate. The housekeeping gene beta-actin (*ACTB*) was used as the most constant endogenous reference control [6]. Raw data was analysed and exported using MxPro QPCR software. Raw fluorescence data was imported to an automated calculation workbook entitled Data Analysis for Real-Time PCR (DART-PCR) which enables rapid calculation of threshold cycles, amplification efficiency and resulting R_0 values (together with the associated error) [28]. Results for each gene were normalized against *ACTB* to obtain the fold change in expression value.

pH measurement

The other halves of carious (n=20) and healthy (n=14) teeth that did not contain pulp were used for pH measurement. Immediately after extraction, the tooth was rinsed and dental plaque carefully removed. None of the patients had dietary carbohydrate exposure within two hours prior to extraction. Four different carious dentin layers were collected from carious teeth using a round steel bur (Premier; USA) at slow speed; the first layer was the superficial soft carious lesion, the second layer was inner soft carious lesion, the third layer comprised caries-affected dentin and the fourth layer, sound dentin beneath the carious lesion and including the reactionary dentin (Fig. 5A). Sound dentin was collected from the crowns of healthy teeth. Each sample was collected in tightly capped tubes and weighed immediately. Measurement of pH was performed [29]. Briefly, weighed samples were suspended in 0.9% NaCl solution at the concentration of 1 mg/4 μl and pH was measured by solid-state metal wire oxide pH sensor (Beetrode; World Precision Instruments, Inc.).

Extraction of dentin proteins

Dentin proteins were extracted by an adaptation and modification of a dentin protein extraction technique [30]. Immediately after pH measurement, each carious layer and sound dentin from healthy tooth samples was used for protein extraction. Pulverized dentin samples were demineralized in 10% EDTA (pH 7.4) with proteinase inhibitors (2.5 mM benzamidine HCl, 50 mM ε-amino-*n*-caproic acid, 0.5 mM *N*-ethyl maleimide, and 0.3 mM phenyl methyl sulphonyl fluoride) for 24 h at 4°C under constant agitation. The first supernatant EDTA (E1) was collected by centrifugation at 2000 *g* for 10 min and stored at −20°C. Demineralized dentin was suspended in 4 M guanidine HCl in 0.05 M TRIS pH 7.4 with proteinase inhibitors for 48 h at 4°C under constant agitation. The first guanidinium chloride extract (G1) was collected by centrifugation at 2000 *g* for 10 min and stored at −20°C. After guanidinium extraction, dentin samples were demineralized in 10% EDTA (pH 7.4) with proteinase inhibitors for 24 h under the same conditions. The second supernatant EDTA (E2) was collected and stored at −20°C. Dentin samples were suspended in 4 M guanidine HCl in 0.05 M TRIS pH 7.4 with proteinase inhibitors for 48 h under the same conditions and the second guanidinium chloride extracts (G2) collected and stored at −20°C. The combination of supernatant EDTA and guanidinium chloride extract (E1+G1+E2+G2) was dialysed by using the 10KDa nominal molecular-weight cut-off (MWCO) Slide-A-Lyzer dialysis cassette (Thermo Scientific; USA) against a large volume of distilled water changed every 12 hours for 3 days at 4°C and then concentrated using an Amicon Ultra-15 centrifugal filter device (Millipore; USA). Total protein yield from each sample was measured spectrophotometrically by Bradford protein assay (Thermo Scientific; USA).

Gelatinase assay

Total gelatinase and specific MMP-2 gelatinase activity was examined for extracted teeth with carious lesions (n=14), from four different layers (Fig 5A) with corresponding controls (n=14) from healthy teeth. Extracted dentin protein (16 μg) from each sample was mixed with 20 μl DQ gelatin (1mg/ml) and reaction buffer to 200 μl final volume in a 96-well white fluorescence plate (Perkin-Elmer) according to the manufacturer's instructions (EnzChek Gelatinase/Collagenase Assay kit; Molecular Probes, Eugene, OR, USA). The assay was run for 24 hr at 37°C and the relative fluorescence recorded at an excitation of 495 nm and emission of 515 nm, background fluorescence was subtracted from all readings. Assays were repeated three times with triplicate samples. MMP-2 gelatinase activity was determined by addition of specific MMP-2 inhibitor I (Calbiochem; San Diago, CA) dissolved in DMSO to 5.05 mg/ml and used in the assay at the reported Ki = 1.7 μM.

Statistical analysis

SPSS statistical software (SPSS v.16; Chicago, Illinois, US) was used for the statistical analysis of data. All data are presented as mean ± SD. Log transformation of data was performed to normalize the distribution of data. Statistical significance was determined by comparison between carious (Pd and Rd) and healthy as a control using a two-tailed Student's *t* test assuming equal variance. In the present study, a *P*-value≤0.05 was considered as statistically significant.

Results

Histological structure of reactionary dentin

Compared with physiologic dentin (Pd) reactionary dentin (Rd) contains fewer, irregular and constricted dentinal tubules as viewed in longitudinal sections (Fig. 1A and 1B). Cross-section of Rd demonstrated the smaller diameter of dentinal tubules compared to the tubules present in Pd (Fig. 1C and 1D).

Analysis of the distribution, area and circularity of dentinal tubules

Low magnification (X6,500) FEI-SEM images from healthy dentin samples showed uniformly distributed round tubules (Fig. 2A). In carious samples, tubules in Pd also present as circular while tubules in Rd (red arrowheads, red tubules and red bars) present as narrow, irregular, randomly distributed structures (Fig. 2B). While dentinal tubules in dentin from healthy teeth and Pd from carious teeth had a high and relatively uniform circularity value, dentinal tubules in Rd showed decreased circularity values (Fig. 2C).

Fractal Analysis of collagen network

The mean lacunarity (λ) and fractal dimensions (D_B) of the collagen networks were calculated for each of nine randomly selected regions of interest [27] from each group (Fig. 3 A-C and Supplementary Table 2).

The FEI-SEM (X20,000) and skeletonized images of the collagen framework in every sample indicated connections between all of the collagen fibrils (Fig. 3A-C). Mean fractal dimension of dentin from healthy teeth (1.76) and Pd (1.76) and Rd (1.72) from carious teeth confirmed a comparable self-similarity level for the collagenous network (Supplementary Table 2). Lacunarity analysis of collagen networks revealed a similar pattern. The mean lacunarity index for the collagen networks in healthy teeth and Pd of carious teeth, was 0.22. The lacunarity index for Rd was slightly higher (0.26) demonstrating decreased rotational symmetry and also a higher cluster of gaps within the collagen framework. However, this difference was not statistically significant (Supplementary Table 2).

Immuno-gold labelling of DSP by ultra-high resolution FEI-SEM

The localisation of DSP, a key component of the mineral phase-interactive acidic matrix [15] was evaluated by immuno-gold labelling. DSP was localized on partially demineralized dentin surfaces of carious and healthy teeth under ultra-high resolution FEI-SEM. A combination of reflected secondary electron and backscattered electron signals (10.00 kV) was applied to simultaneously reveal immuno-gold labelling and related substrate morphology. Positive labelling was indicated by white spherical spots of ~20 nm diameter. DSP was localized in dentin of healthy teeth (Fig. 4A) and both Pd (Fig. 4B) and Rd (Fig. 4C) of carious teeth. At high magnification (X95,000), DSP was closely associated with the collagen network (Fig. 4A-C). Plot Profile displays were used to analyse the distribution of DSP. Twelve randomly selected areas from three samples in each group were analysed. DSP

was densely deposited in Rd whereas DSP in Pd and in dentin from healthy teeth was more sparsely distributed (Fig. 4A-C). A density bar chart (using Measure analysis tool ImageJ version 1.41o; National Institutes of Health) confirmed this pattern of distribution (Fig. 4D).

MMP-2 and gelatinase activity in dentin layers

The dentin protein extracted from all dentin layers had detectable gelatinase activity. Rd (layer 4) had total gelatinolytic activity of 0.38 ± 0.11 relative fluorescence units (RFU) per μg of total protein and specific MMP-2 gelatinolytic activity of 0.31 ± 0.08 RFU/μg. Dentin protein extracted from healthy teeth contained total gelatinolytic activity of 0.06 ± 0.02 RFU/μg all of which was contributed by MMP-2 (Fig. 5B). A collagenase standard curve was generated using dilutions of *Clostridium histolyticum* (0 - 0.0012 U/μl) to cleave fluorescein-gelatin (Fig. 5C). The activity of MMP-2 present in each dentin layer was calculated by plotting to the standard curve according to the instruction of manufacturer. The protein extracted from Rd (layer 4) contained specific MMP-2 activity of 19.36 ± 5.13 mU/μg while protein extracted from healthy dentin samples contained specific MMP-2 activity of 3.50 ± 0.12 mU/μg (Fig. 5C). This finding was in agreement with the localization of MMP-2 by immunohistochemistry. MMP-2 was detected within dentinal tubules containing odontoblastic processes. More intense reactivity for MMP-2 was detected in the Rd compared to the comparable layer of dentin from healthy teeth (Fig. 5D).

Bacteria invasion and pH distribution in the carious lesion

Localization of bacteria correlated with destruction of dentin exposed to organic acid products of bacterial metabolism. Disruption of the dentin-enamel junction and widening of affected dentinal tubules was observed (Fig. 6A). Accumulation of bacteria in the dentin-enamel junction and penetration of bacteria through dentinal tubules was detected by FISH (Fig. 6B). Dentin samples from four different layers of carious teeth were sampled for pH measurement. Twenty carious and fourteen healthy teeth were analysed. The pH measurements demonstrated a gradual rise from 5.60 at the most superficial layer to 6.50 in the deepest site corresponding to reactionary dentin while dentin from healthy teeth had a pH of 7.68 (Fig. 6C).

Analysis of matrix-forming capacity of odontoblasts

The response of odontoblasts adjacent to carious lesions was compared to the corresponding region from healthy teeth (Fig. 7A). Genes encoding both MMP-2 and TIMP-2 were significantly up-regulated in odontoblasts adjacent to the carious front (Fig. 7B). Marked up-regulation of *MT1-MMP* in odontoblasts adjacent to the carious front paralleled up-regulation of *TIMP-2* expression (Fig. 7B). There is evidence that MT1-MMP and Endo180, a membrane-bound receptor that is able to bind collagen fragments for subsequent endocytic uptake, are key mediators of the remodelling of collagen in patho-physiological conditions [31, 32]. We first performed a fluorescence immunohistochemical investigation of MT1-MMP and Endo180 in the odontoblastic layer from healthy and carious teeth. Strong labelling for MT1-MMP in odontoblastic layers of carious teeth was observed, with weaker signal in the odontoblastic layer from healthy teeth. In contrast, labelling for Endo180 was intense in the odontoblastic layer from healthy teeth but barely detectable in carious teeth (Fig. 7C), correlating with corresponding data for gene expression (Fig. 7B).

SMAD-2 and -4 are proteins involved in signalling following receptor ligation by TGF-β [33]. Significant up-regulation of *SMAD-2* and *-4* was detected in the odontoblastic layer of carious teeth. Genes encoding collagen type Iα1 and collagen type Iα2, comprising the scaffold for mineralized tissue [34], were also up-regulated in carious teeth (Fig. 7D).

Genes encoding TLR-4 and the corresponding adaptor proteins, TRAM and Mal/TIRAP were markedly up-regulated in the odontoblast layer adjacent to the carious front while *TLR-2* and corresponding adaptor component *MyD88* were down-regulated (Fig. 7D). Further, expression for the transcription factor *NF-κB* was up-regulated while expression for the inhibitor *IκBα* was down-regulated in the odontoblast layer adjacent to the carious front (Fig. 7D).

Discussion

The aim of the present study was to investigate the structure of reactionary dentin with reference to the collagen framework of dentin and the regulation of DSP deposition. The main findings are displayed in Figure 8 and can be summarized as:

- The collagen framework of reactionary dentin is modified and yet highly regular, patterned and non-stochastic. The altered collagen network parallels increased deposition of DSP as a putative calcium nucleation site.
- Synthesis by odontoblasts of the highly altered reactionary dentin matrix necessitates modulation of the associated enzymatic machinery, potentially mediated, at least in part, by a switch in expression of TLRs.

Reactionary dentin is characterised by an altered tubular structure and diminished tubularity. Deposition by odontoblasts of a relatively atubular reactionary dentin is an efficient strategy to impede or delay microbial progression, evident from the protracted nature of dental caries [8]. While modified, the synthesis of reactionary dentin matrix is not a stochastic process. Assessment of fractal dimensions and lacunarity of the collagen network of reactionary dentin indicated an orderly and structured pattern which clearly contrasts with increased fractal dimensionality of trabecular bone in inflammatory joint disease [35]. The latter is mainly a direct outcome of the inflammatory response whereas reactionary dentin is an adaptive phenotype actively synthesized by radically re-programmed odontoblasts in a non-inflammatory context. The functional re-programming of odontoblasts parallels the modulation of the synthesis of dentin matrix components and associated enzymatic repertoire by odontoblasts.

The extracellular matrix (ECM) of mineralized tissues contains three groups of components. The structural matrix macromolecules, such as collagen, determine the shape and the structure of the mineralized component. Mineral phase-interactive acidic matrix proteins intermediate between collagen and mineral by regulating the site of initial crystal deposition and the type of mineral crystal deposited [36]. In bone and dentin, phosphoproteins are the dominant group. Finally, modifier proteinases and other enzymes have the capacity to degrade or modify the acidic matrix proteins during the mineralization process.

DSP, an important NCP, influences the location of mineral crystal formation [37]. Dense DSP labelling observed on the collagen fibrils in reactionary dentin is concordant with a previous report indicating marked up-regulation of *DSPP* during reactionary dentinogenesis [6]. Increased deposition of DSP suggests a modified crystallization process with amplified putative hydroxyapatite nucleation sites, in reactionary dentinogenesis. Higher density of DSP detected in reactionary dentin is compatible with increased expression and activity of MMP-2. As the pH in reactionary dentin was too high for the activation of MMP-2 (pH 6.49) [38], it is likely that the activation of MMP-2 was mediated by MT1-MMP, shown to be markedly up-regulated in response to caries. In support of the role of MMP-2 in reactionary dentinogenesis, it has been reported that MMP-2 knockout mice demonstrate delayed formation of mineralized tissues, including dentin and bone, during post-natal development [39]. In addition, loss of MMP-2 reduces mineralization density and tissue hardness [40].

Up-regulation of message for MT1-MMP by odontoblasts adjacent to caries parallels down-regulated expression of Endo180. MT1-MMP expression is essential for post-natal tissue remodelling [41, 42] and mice deficient in MT1-MMP have delayed formation of mineralized tissue [27, 43]. MT1-MMP potently activates latent pro-MMP-2 by binding to TIMP-2 [44]. Down-regulation of *Endo180*, encoding a novel collagen-binding and collagen internalisation receptor, has been reported to increase MT1-MMP activity and consequentially, activate MMP-2 [45], a finding compatible with the data obtained for carious teeth.

Odontoblasts express Toll-like receptors which recognize pathogen-associated molecular patterns [46, 47]. The response to microbial invasion of dentin was marked by potent up-regulation of TLR-4 and associated adaptor proteins. In particular, TLR-4 recognizes lipopolysaccharide, a common product of Gram negative bacteria found consistently in carious dentin [48, 49]. In addition, products released from tissue damage including fibronectin extra domain A fragment, heat shock proteins and hyaluronan fragments can also be recognized by TLRs [50]. The expression of Mal/TIRAP is important in regulating expression of MMP-2 [51]. TLRs regulate the innate immune response via their adaptor proteins and the NF-κB pathway [52]. NF-κB regulates transcription of DNA, and is usually present in cells in a latent state by binding with IκBα, the inhibitor. NF-κB can be activated without requiring protein synthesis [53] although up-regulation of the gene encoding NF-κB and down-regulation of the gene encoding IκBα was observed in response to caries. A shift in the balance between NF-κB and IκBα results in the activation of NF-κB [54]. Prolonged activation of TLRs results in hypo-responsiveness to subsequent ligand stimulation, a phenomenon termed TLR tolerance [55]. This could be one reason for the down-regulation of genes encoding TLR-2 and MyD88, important for recognition of Gram positive bacteria that dominate the early stage of this chronic infection.

The up-regulation of gene expression for collagen type Iα1 and α2 could be induced by the TGF-β signalling cascade [56, 57]. In this regard, while expression of *TGF-β1* in the odontoblast layer is down-regulated during carious progression [6], expression for TGF-β signalling pathway components *SMAD-2* and *-4* was up-regulated. A potential exogenous source of TGF-β released from demineralized dentin during carious progression could explain activation of the TGF-β signalling cascade [58]. Extracellular and pericellular collagen is remodelled by MMPs, particularly MT1-MMP [42]. A collagen-binding and internalisation receptor, endocytic receptor (Endo180), also binds collagen fragments for uptake via clathrin-coated pits into early endosomes for lysosomal degradation [59, 60]. This is compatible with our data demonstrating up-regulation of *MT1-MMP* and down-regulation of *Endo180* during the formation of reactionary dentin.

Present findings highlight the roles of matrix proteins, collagenous and noncollagenous, and matrix remodelling enzymes particularly MMP-2, in the formation of altered reactionary dentin matrix. Notably, MMP-2 is involved in bone formation and remodelling and mutations in *MMP-2* cause multicentric osteolysis or “vanishing bone” disease, characterized by marked and progressive bone loss and joint destruction [61]. In reactionary dentinogenesis, MMP-2 is likely to facilitate the release of DSP from DSPP. Mutations of *DSPP* have been implicated in pathogenesis of dentin dysplasia type II, dentinogenesis imperfecta type I associated with osteogenesis imperfecta [5] and dentinogenesis imperfecta type II and III [62].

The present study has defined essential parameters of the response of the dental pulp to microbial invasion of dentin. Findings indicate a consistent adaptive change in odontoblast synthetic activity leading to the formation of a modified calcified matrix that effectively impedes migration of bacteria along the dentinal tubules, thereby protecting the dental pulp

from invasion. The uniformity of this response despite inevitable variation in lesion stage and microbial etiology, strongly suggests activation of an alternative program for establishing calcified matrix. This research provides a basis for further investigation leading to improved therapeutic protocols for advanced caries.

Supplementary Material

Refer to Web version on PubMed Central for supplementary material.

Acknowledgments

NC would like to thank Mary Simonian, Ky-ahn Nguyen and Luiz E. Bertassoni for valuable technical assistance and discussion. Scanning electron microscopy was performed with assistance from staff at the Australian Microscopy & Microanalysis Research Facility, at The University of Sydney. This work was supported by a grant to NH from the National Institutes of Health (R01 DEO15272-07) and a grant to NC from the Australian Dental Research Foundation (37/2010). NC was supported by a Naresuan University Thailand Staff Development Project scholarship.

Funding Source: National Institutes of Health (R01 DEO15272-07) and the Australian Dental Research Foundation (37/2010).

References

[1]. Goldberg M, Septier D, Lecolle S, Chardin H, Quintana MA, Acevedo AC, Gafni G, Dillouya D, Vermelin L, Thonemann B, et al. Dental mineralization. Int J Dev Biol. 1995; 39:93–110. [PubMed: 7626424]

[2]. Butler WT, Brunn JC, Qin C. Dentin extracellular matrix (ECM) proteins: comparison to bone ECM and contribution to dynamics of dentinogenesis. Connect Tissue Res. 2003; 44(Suppl 1): 171–8. [PubMed: 12952193]

[3]. Kawasaki K, Weiss KM. Mineralized tissue and vertebrate evolution: the secretory calcium-binding phosphoprotein gene cluster. Proc Natl Acad Sci U S A. 2003; 100:4060–4065. [PubMed: 12646701]

[4]. Donoghue PC, Sansom IJ, Downs JP. Early evolution of vertebrate skeletal tissues and cellular interactions, and the canalization of skeletal development. J Exp Zool B Mol Dev Evol. 2006; 306:278–294. [PubMed: 16555304]

[5]. Xiao S, Yu C, Chou X, Yuan W, Wang Y, Bu L, Fu G, Qian M, Yang J, Shi Y, Hu L, Han B, Wang Z, Huang W, Liu J, Chen Z, Zhao G, Kong X. Dentinogenesis imperfecta 1 with or without progressive hearing loss is associated with distinct mutations in DSPP. Nat Genet. 2001; 27:201–4. [PubMed: 11175790]

[6]. Farahani RM, Nguyen KA, Simonian MR, Hunter N. Adaptive calcified matrix response of dental pulp to bacterial invasion is associated with establishment of a network of glial fibrillary acidic protein^{+}/Glutamine Synthetase^{+} Cells. Am J Pathol. 2010; 177:1901–1914. [PubMed: 20802180]

[7]. Chhour KL, Nadkarni MA, Byun R, Martin FE, Jacques NA, Hunter N. Molecular analysis of microbial diversity in advanced caries. J Clin Microbiol. 2005; 43:843–9. [PubMed: 15695690]

[8]. Smith AJ, Cassidy N, Perry H, Begue-Kirn C, Ruch JV, Lesot H. Reactionary dentinogenesis. Int J Dev Biol. 1995; 39:273–80. [PubMed: 7626417]

[9]. Boskey AL. Noncollagenous matrix proteins and their role in mineralization. Bone Miner. 1989; 6:111–23. [PubMed: 2670018]

[10]. Linde A, Bhown M, Butler WT. Noncollagenous proteins of dentin. A re-examination in proteins from rat incisor dentin utilizing techniques to avoid artifacts. J Biol Chem. 1980; 255:5931–5942. [PubMed: 7380844]

[11]. Yamakoshi Y, Hu JC, Fukae M, Zhang H, Simmer JP. Dentin glycoprotein: The protein in the middle of the dentin Sialophosphoprotein chimera. J Biol Chem. 2005; 280:17472–17479. [PubMed: 15728577]

[12]. Qin C, Brunn JC, Cadena E, Ridall A, Tsujigiwa H, Nagatsuka H, Nagai N, Butler WT. The expression of dentin sialoprotein gene in bone. J Dent Res. 2002; 81:392–394. [PubMed: 12097430]

[13]. Baba O, Qin C, Brunn JC, Jones JE, Wygant JN, Mclntyre BW, Butler W. Detection of dentin sialoprotein in rat periodontium. Eur J Oral Sci. 2004a; 112:163–170. [PubMed: 15056114]

[14]. Yamakoshi Y, Hu JC, Iwata T, Kobayashi K, Fukae M, Simmer JP. Dentin Sialophosphoprotein Is Processed by MMP-2 and MMP-20 in Vitro and in Vivo. J Biol Chem. 2006; 281:38235–38243. [PubMed: 17046814]

[15]. Prasad M, Butler WT, Qin C. Dentin Sialophosphoprotein (DSPP) in Biomineralization. Connect Tissue Res. 2010; 51:404–417. [PubMed: 20367116]

[16]. D'Angelo M, Billings PC, Pacifici M, Leboy PS, Kirsch T. Authentic matrix vesicles contain active metalloproteases (MMP). a role for matrix vesicle-associated MMP-13 in activation of transforming growth factor-beta. J Biol Chem. 2001; 276:11347–11353. [PubMed: 11145962]

[17]. Nagase H, Woessner JF. Matrix metalloproteinases. J Biol Chem. 1999; 274:21491–21494. [PubMed: 10419448]

[18]. Meikle MC, Bord S, Hembry RM, Compston J, Croucher PI, Reynolds JJ. Human osteoblasts in culture synthesize collagenase and other matrix metalloproteinases in response to osteotropic hormones and cytokines. J Cell Sci. 1992; 103:1093–1099. [PubMed: 1336777]

[19]. Rifas L, Halstead LR, Peck WA, Avioli LV, Welgus HG. Human osteoblasts in vitro secrete tissue inhibitor of metalloproteinases and gelatinase but not interstitial collagenase as major cellular products. J Clin Invest. 1989; 84:686–694. [PubMed: 2547836]

[20]. Palosaari H, Wahlgren J, Larmas M, Ronka H, Sorsa T, Salo T, Tjäderhane L. The expression of MMP-8 in odontoblasts and dental pulp cells is down-regulated by TGF-β1. J Dent Res. 2000; 79:77–84. [PubMed: 10690664]

[21]. Mazzoni A, Mannello F, Tay FR, Tonti GAM, Suppa P, Papa S, Mazzotti G, Lenarda R.Di, Pashley DH, Breschi L. Zymographic analysis and characterization of MMP-2 and -9 isoforms in human sound dentin. J Dent Res. 2007; 86:436–440. [PubMed: 17452564]

[22]. Wang M, Zhao D, Spinetti G, Zhang J, Jiang LQ, Pintus G, Monticone R, Lakatta EG. Matrix Metalloproteinase 2 Activation of Transforming Growth Factor-ß1 (TGF-ß1) and TGF-ß1–Type II Receptor Signaling Within the Aged Arterial Wall. AHA Journals. 2006; 26:1503–1509.

[23]. Gilles C, Polette M, Seiki M, Birembaut P, Thompson EW. Implication of collagen type-1 induced membrane-type 1-matrix metalloproteinase expression and matrix metalloproteinase-2 activation in the metastatic progression of breast carcinoma. Lab Invest. 1997; 76:651–660. [PubMed: 9166284]

[24]. Kurschat P, Zigrino P, Nischt R, Breitkopf K, Steurer P, Klein EC, Krieg T, Mauch C. Tissue inhibitor of matrix metalloproteinase-2 regulates matrix metalloproteinase-2 activation by modulation of membrane-type 1 matrix metalloproteinase activity in high and low invasive melanoma cell lines. J Biol Chem. 1999; 274:21056–21062. [PubMed: 10409657]

[25]. Nadkarni MA, Simonian MR, Harty DW, Zoellner H, Jacques NA, Hunter N. Lactobacilli are prominent in the initial stages of polymicrobial infection of dental pulp. J Clin Microbiol. 2010; 48:1732–1740. [PubMed: 20200294]

[26]. Bedran-Russo AKB, Pereira PNR, Duarte WR, Okuyama K, Yamauchi M. Removal of dentin matrix proteoglycans by trypsin digestion and its effect on dentin bonding. J Biomed Mater Res B. 2007; 85B:261–266.

[27]. Geoffroy V, Marty-Morieux C, Le Goupil N, Clement-Lacroix P, Terraz C, Frain M, Roux S, Rossert J, Vernejoul MC. In vivo inhibition of osteoblastic metalloproteinases leads to increased trabecular bone mass. J Bone Miner Res. 2004; 19:811–822. [PubMed: 15068505]

[28]. Peirson SN, Butler JN, Foster RG. Experimental validation of novel and conventional approaches to quantitative real-time PCR data analysis. Nucleic Acids Res. 2003; 31:e73. [PubMed: 12853650]

[29]. Hojo S, Komatsu M, Okuda R, Takahashi N, Yamada T. Acid profiles and pH of carious dentin in active and arrested lesions. J Dent Res. 1994; 73:1853–1857. [PubMed: 7814758]

[30]. Martin-De Las Heras S, Valenzuela A, Overall CM. The matrix metalloproteinase gelatinase A in human dentine. Arch Oral Biol. 2000; 45:757–765. [PubMed: 10869489]

[31]. Curino AC, Engelholm LH, Yamada SS, Holmbeck K, Lund LR, Molinolo AA, Behrendt N, Nielsen BS, Bugge TH. Intracellular collagen degradation mediated by uPARAP/Endo180 is a major pathway of extracellular matrix turnover during malignancy. J Cell Biol. 2005; 169:977–985. [PubMed: 15967816]

[32]. Ye Q, Xing Q, Ren Y, Harmsen MC, Bank RA. Endo180 and MT1-MMP are involved in the phagocytosis of collagen scaffolds by macrophages and is regulated by interferon-gamma. Eur Cell Mater. 2010; 7:197–209. [PubMed: 20931490]

[33]. Nakao A, Imamura T, Souchelnytskyi S, Kawabata M, Ishisaki A, Oeda E, Tamaki K, Hanai JI, Heldin CH, Miyazono K, Dijke PT. TGF- receptor-mediated signalling through Smad2, Smad3 and Smad4. EMBO. 1997; 16:5353–5362.

[34]. Gelse K, Poschl E, Aigner T. Collagens—structure, function, and biosynthesis. Adv Drug Deliv Rev. 2003; 55:1531–1546. [PubMed: 14623400]

[35]. Caldwell CB, Moran EL, Bogoch ER. Fractal dimension as a measure of altered trabecular bone in experimental inflammatory arthritis. J Bone Miner Res. 1998; 13:978–85. [PubMed: 9626629]

[36]. Addadi L, Weiner S. Interactions between acidic proteins and crystals: stereochemical requirements in biomineralization. Proc Natl Acad Sci U S A. 1985; 82:4110–4114. [PubMed: 3858868]

[37]. Veis A. Mineral-matrix interactions in bone and dentine. J Bone Miner Res. 1993; 8:493–497.

[38]. Tjäderhane L, Larjava H, Sorsa T, Uitto VJ, Larmas M, Salo T. The activation and function of host matrix metalloproteinase in dentin matrix breakdown in caries lesions. J Dent Res. 1998; 77:1622–1629. [PubMed: 9719036]

[39]. Itoh T, Tomioka M, Yoshida H, Yoshioka T, Nishimoto H, Itohara S. Reduced angiogenesis and tumor progression in gelatinase A-deficient mice. Cancer Res. 1998; 58:1048–1051. [PubMed: 9500469]

[40]. Nyman JS, Lynch CC, Perrien DS, Thiolloy S, O′Quinn EC, Patil CA, Bi X, Pharr GM, Mahadevan JA, Mundy GR. Differential effects between the loss of MMP-2 and MMP-9 on structural and tissue-level properties of bone. J Bone Miner Res. 2011; 26:1252–1260. [PubMed: 21611966]

[41]. Holmbeck K, Bianco P, Caterina J, Yamada S, Kromer M, Kuznetsov SA, Mankani M, Robey PG, Poole AR, Pidoux I, Ward JM, Birkedal-Hansen H. MT1-MMP-deficient mice develop dwarfism, osteopenia, arthritis, and connective tissue disease due to inadequate collagen turnover. Cell. 1999; 99:81–92. [PubMed: 10520996]

[42]. Holmbeck K, Bianco P, Pidoux I, Inoue S, Billinghurst RC, Wu W, Chrysovergis K, Yamada S, Birkedal-Hansen H, Poole AR Robin. The metalloproteinase MT1-MMP is required for normal development and maintenance of osteocyte processes in bone. J Cell Sci. 2004; 118:147–156. [PubMed: 15601659]

[43]. Holmbeck K, Bianco P, Yamada S, Birkedal-Hansen H. MT1-MMP: a tethered collagenase. J Cell Physiol. 2004; 200:11–19. [PubMed: 15137053]

[44]. Strongin AY, Cillier I, Bannikov G, Marmer BL, Grant GA, Goldberg GI. Mechanism of cell surface activation of 72 kDa type IV collagenase. J Biol Chem. 1995; 270:5331–5338. [PubMed: 7890645]

[45]. Messaritou G, East L, Roghi C, Isacke CM, Yarwood H. Membrane type-1 matrix metalloproteinase activity is regulated by the endocytic collagen receptor Endo180. J Cell Sci. 2009; 122:4042–4048. [PubMed: 19861500]

[46]. Mutoh N, Tani-Ishii N, Tsukinoki N, Chieda K, Watanabe K. Expression of toll-like receptor 2 and 4 in dental pulp. J Endod. 2007; 33:1183–6. [PubMed: 17889686]

[47]. Hahn CL, Liewehr FR. Innate Immune Responses of the Dental Pulp to Caries. J Endod. 2007; 33

[48]. Hoshino E. Predominant obligate anaerobes in human carious dentin. J Dent Res. 1985; 64:1195–1198. [PubMed: 3861648]

[49]. Martin FE, Nadkarni MA, Jacques NA, Hunter N. Quantitative microbiological study of human carious dentine by culture and realtime PCR: association of anaerobes with histopathological changes in chronic pulpitis. J Clin Microbiol. 2002; 40:1698–1704. [PubMed: 11980945]

[50]. Rifkin IR, Leadbetter EA, Busconi L, Viglianti G, Marshak-Rothstein A. Toll-like receptors, endogenous ligands, and systemic autoimmune disease. Immunol Rev. 2005; 204:27–42. [PubMed: 15790348]

[51]. Sacre SM, Andreakos E, Kiriakidis S, Amjadi P, Lundberg A, Giddins G, Feldmann M, Brennan F, Foxwell BM. The toll-like receptor adaptor proteins MyD88 and Mal/TIRAP contribute to the Inflammatory and destructive processes in a human model of rheumatoid arthritis. Am J Pathol. 2007; 170:518–525. [PubMed: 17255320]

[52]. Carmody RJ, Ruan Q, Palmer S, Hilliard B, Chen YH. Negative regulation of toll-like receptor signaling by NF-κB p50 ubiquitination blockade. Science. 2007; 317:675–678. [PubMed: 17673665]

[53]. Ramirez-Carrozzi VR, Nazarian AA, Li CC, Gore SL, Sridharan R, Imbalzano AN, Smale ST. Selective and antagonistic functions of SWI/SNF and Mi-2β nucleosome remodeling complexes during an inflammatory response. Genes Dev. 2006; 20:282–296. [PubMed: 16452502]

[54]. Pennington KN, Taylor JA, Bren GD, Paya CV. IκB kinase-dependent chronic activation of NF-κB is necessary for p21WAF1/Cip1 inhibition of differentiation-induced apoptosis of monocytes. Mol Cell Biol. 2001; 21:1930–1941. [PubMed: 11238929]

[55]. Medvedev AE, Sabroe I, Hasday JD, Vogel SN. Tolerance to microbial TLR ligands: molecular mechanisms and relevance to disease. J Endotoxin Res. 2006; 12:133–150. [PubMed: 16719986]

[56]. Chen TL, Bates RL. Recombinant human transforming growth factor beta 1 modulates bone remodeling in a mineralizing bone organ culture. J Bone Miner Res. 1993; 8:423–434. [PubMed: 8475792]

[57]. Nie X, Tian W, Zhang Y, Chen X, Dong R, Jiang M, Chen F, Jin Y. Induction of transforming growth factor-beta 1 on dentine pulp cells in different culture patterns. Cell Biol Int. 2006; 30:295–300. [PubMed: 16458025]

[58]. Tziafas D, Papadimitriou S. Role of exogenous TGF-beta in induction of reparative dentinogenesis in vivo. Eur J Oral Sci. 1998; 106(Suppl1):192–196. [PubMed: 9541225]

[59]. Engelholm LH, List K, Netzel-Arnett S, Cukierman E, Mitola DJ, Aaronson H, Kjeller L, Larsen JK, Yamada KM, Strickland DK, Holmbeck K, Dane K, Birkedal-Hansen H, Behrendt N, Bugge TH. uPARAP/Endo180 is essential for cellular uptake of collagen and promotes fibroblast collagen adhesion. J Cell Biol. 2003; 160:1009–1015. [PubMed: 12668656]

[60]. Kjoller L, Engelholm LH, Hoyer-Hansen M, Dano K, Bugge TH, Behrendt N. uPARAP/endo180 directs lysosomal delivery and degradation of collagen IV. Exp Cell Res. 2004; 293:106–116. [PubMed: 14729061]

[61]. Mosig RA, Dowling O, DiFeo A, Ramirez MCM, Parker IC, Abe E, Diouri J, Aqeel AA, Wylie JD, Oblander SA, Madri J, Bianco P, Apte SS, Zaidi M, Doty SB, Majeska RJ, Schaffler MB, Martignett JA. Loss of MMP-2 disrupts skeletal and craniofacial development and results in decreased bone mineralization, joint erosion and defects in osteoblast and osteoclast growth. Hum Mol Genet. 2007; 16:1113–1123. [PubMed: 17400654]

[62]. Yamakoshi Y. Dentinogenesis and Dentin Sialophosphoprotein (DSPP). J Oral Biosci. 2009; 51:134. [PubMed: 20157636]

Highlights

- *TLR-2* and *-4* expression was differentially expressed in the odontoblastic layer in healthy and carious teeth.
- In carious teeth, *MMP-2* was up-regulated, accompanied by up-regulation of *MT1-MMP* resulting in activated MMP-2 found in reactionary dentin.
- DSP was significantly more densely deposited on newly synthesised collagen framework in reactionary dentin.
- Assessment of fractal dimensions and lacunarity of the collagen network of reactionary dentin indicated an orderly and structured pattern.
- Significant up-regulation of *SMAD-2* and *-4* was detected in carious teeth without up-regulation of *TGF-β* from the odontoblastic layer.

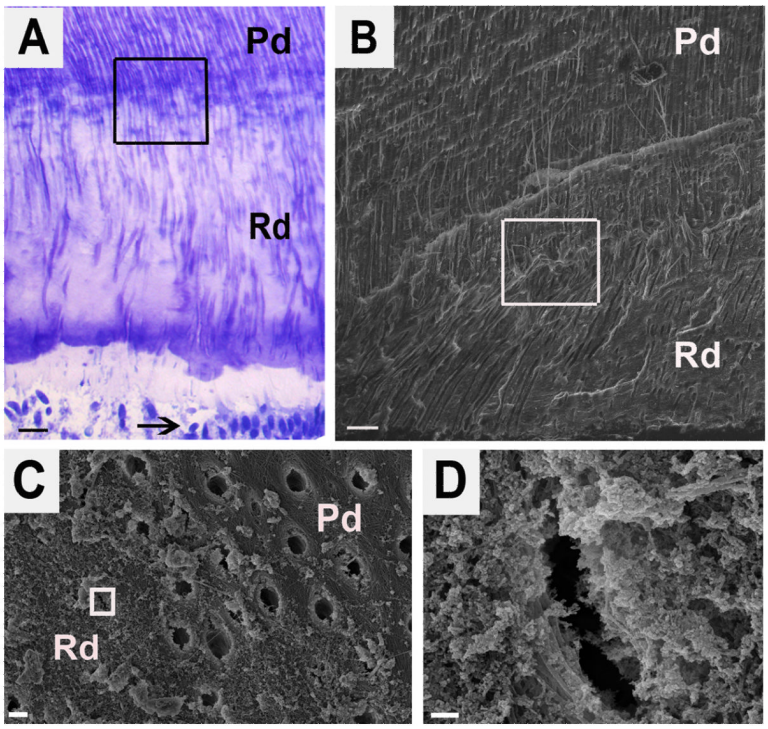

Figure 1.

Structure of reactionary dentin demonstrating fewer tubules that are more irregular and constricted. (A) Toluidine blue stain of longitudinal section of reactionary dentin. Pd and Rd indicate the area of physiologic dentin and reactionary dentin, respectively. Arrow points to odontoblasts. The boxed area encompasses the boundary between Pd and Rd. Scale bar 20 μm. (B) Scanning electron micrograph (SE detector at 10.00 kV, X500) of the boxed area from A. Scale bar 20 μm. (C) Scanning electron micrograph (SE detector at 10.00 kV, X7,500) of a cross-section of the boxed area from B and showing the boundary between Pd and Rd. Scale bar 2 μm. (D) A high magnification view (SE detector at 10.00 kV, X60,000) of the boxed area from C showing the morphology of a constricted tubule in the Rd. Scale bar 200 nm.

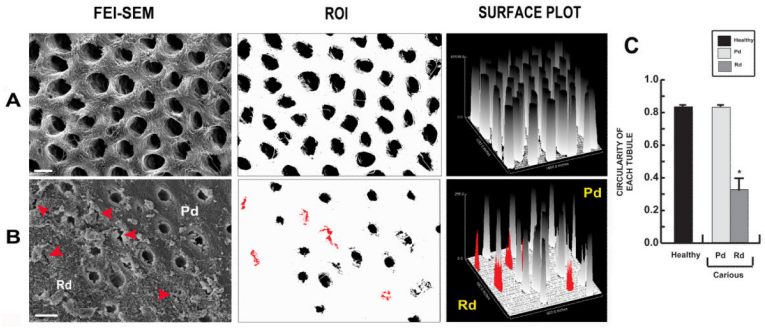

Figure 2.

Representative images demonstrating the distribution, area and circularity of dentinal tubules in healthy and carious samples. (A) Cross-sectional view of dentinal tubules from dentin in a healthy tooth. Large circular and uniformly distributed tubules are observed (first and second panels). Scale bar 2 μm. Findings were confirmed by analysis of a Surface plot (third panel). (B) Dentinal tubules in carious sample. For Pd, the tubules present similar characteristics to dentin of healthy teeth while tubules in Rd (red arrowheads, red tubules and red bars) present as narrow, irregular cross-section with random distribution (first and second panels). Scale bar 2 μm. Surface plot analysis confirmed similar patterns for Pd compared to dentin from healthy teeth whereas Rd presents as variable, in both tubular area and distribution of tubules (third panel). (C) Bar graph representing the circularity of tubules in each region (n=30). Tubules in dentin of healthy teeth and in Pd of carious teeth present similar profiles with a circularity index close to 1, representative of a circle. In Rd the circularity of tubules is low reflecting irregular shape. The data for circularity are expressed as mean values ± SD. * $P \leq 0.05$.

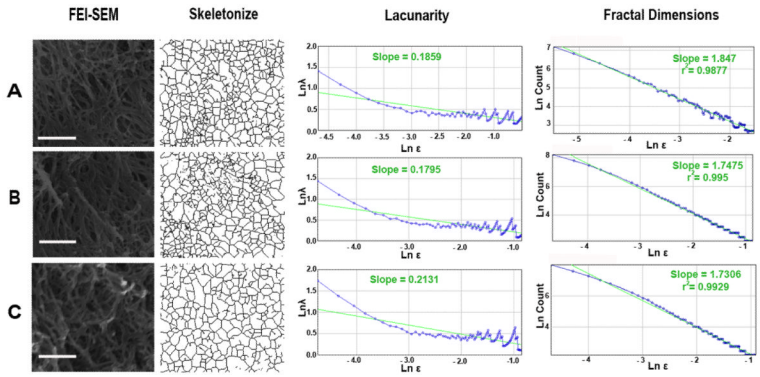

Figure 3.

Representative images demonstrate the collagen frameworks in healthy and carious samples. (A) Collagen framework in healthy sample displays connection between the fibrils with the slope of lacunarity of 0.1859 and the slope of fractal dimensions of 1.847. (B) Collagen framework in Pd from carious sample also presents connection between the fibrils with the slope of lacunarity of 0.1795 and the slope of fractal dimensions of 1.7475. (C) In Rd the connection between collagen fibrils can be observed with the slope of lacunarity of 0.2131 and the slope of fractal dimensions of 1.7306. Scale bar 1 μm.

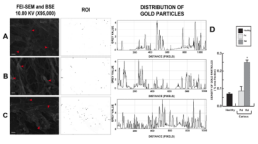

Figure 4.

Representative images of immunogold-labelling of DSP on fixed partially demineralized dentin. (A) DSP labelling (arrowheads) were observed on the collagen fibrils in dentin from healthy tooth with a random distribution pattern. (B) In carious teeth DSP localisation in Pd closely follows that observed in dentin from healthy teeth. (C) Rd demonstrates the densest pattern of distribution. Scale bars 200 nm. Bar chart demonstrating the density of DSP in terms of percentage of area fraction. Rd area has the densest DSP labelling compared to Pd area and dentin from healthy teeth (n=12). The data for density of DSP labelling are expressed as mean values ± SD. * $P \leq 0.05$.

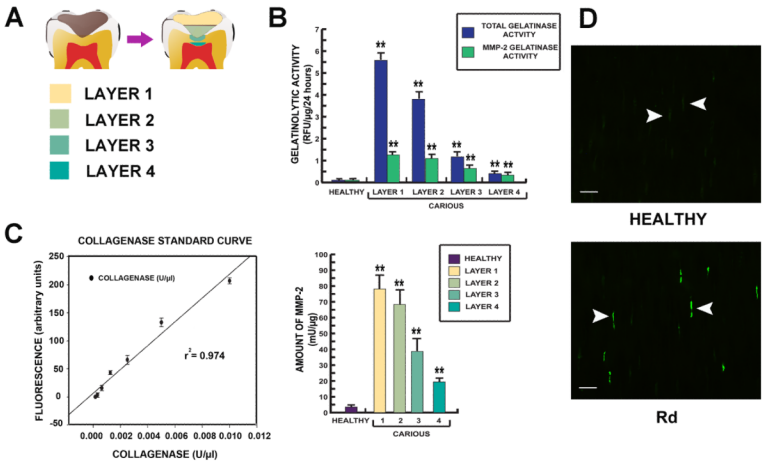

Figure 5.

Data demonstrating the gelatinase activity of MMP-2 in each dentin layer. (A) Diagram of dentin layers; layer 1 the superficial soft carious lesion, layer 2 inner soft carious lesion, layer 3 caries-affected dentin and layer 4 sound dentin beneath carious lesion including Rd. (B) Bar charts demonstrating gelatinolytic activity from extracted total dentin protein from each dentin layer. Gelatinolytic activity detected in Rd (layer 4) was almost entirely contributed by MMP-2. The activity was 5 times higher than gelatinolytic activity detected in the corresponding layer of dentin from healthy teeth. (C) MMP-2 activity in each dentin layer was calculated from a collagenase standard curve of the gelatin-fluorescein conjugate cleaved by *Clostridium histolyticum*. MMP-2 activity in the Rd (layer 4) was significantly higher than the healthy sample. All values depict means ± SD (n=14). * $P \leq 0.05$; ** $P \leq 0.02$. (D) Demonstration of MMP-2 expression in dentinal tubules in the Rd area by immunofluorescence on a semi-thin resin section. Positive labelling is indicated by bright green fluorescence. Staining for MMP-2 (arrowheads) observed in some dentinal tubules in the area of Rd was more abundant and intense compared to dentin from healthy teeth. Scale bar 20 µm.

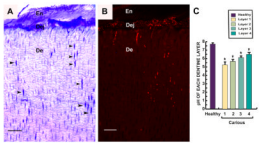

Figure 6.

Semi-thin resin sections perpendicular to tooth axis of a carious tooth showing invasion of bacteria from enamel (En) through the dentin-enamel junction (Dej) and into dentin (De). (A) Toluidine blue stain demonstrates invasion of bacteria along dentinal tubules (arrowheads). (*B*) Fluorescence *in situ* hybridization (FISH) with a universal 16SrRNA bacterial probe. Red fluorescence shows bacteria accumulating along the Dej and in dentinal tubules. Scale bar 30 μm. (C) Bar chart demonstrates pH gradient in different layers (Fig. 5A) from carious teeth (n=20) compared to healthy teeth (n=14). In the area of the infected soft carious lesion (layers 1&2), the pH was low increasing progressively in the deeper layers. Values depicted mean values ± SD. **P*≤ 0.05

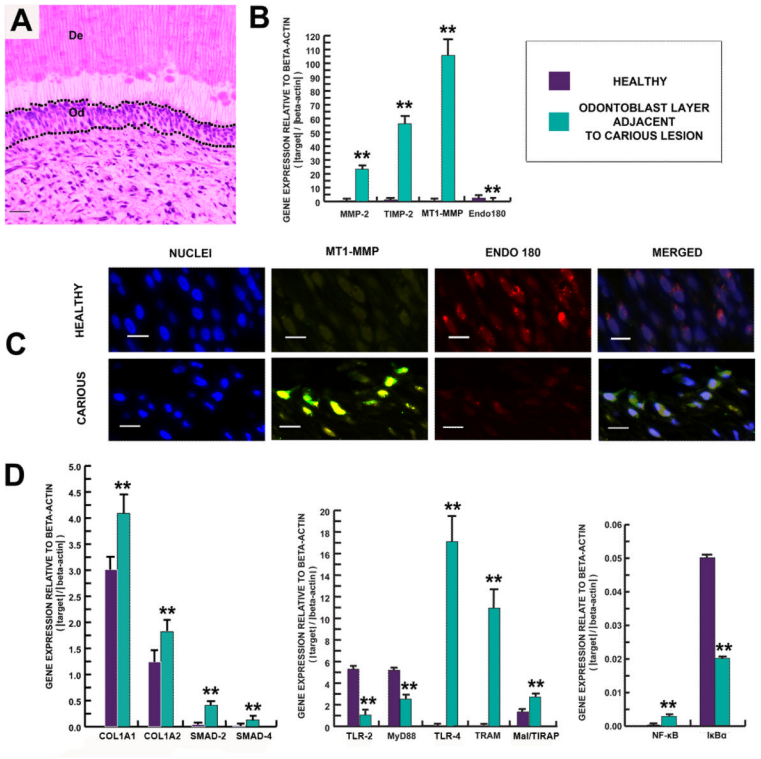

Figure 7.

The synthetic activity of the odontoblast layer changes in response to carious stimuli. (A) Toluidine blue staining demonstrates micro-dissection of the odontoblast layer (Od). Scale bar 20 μm. (B) Bar chart demonstrating up-regulation of *MMP-2*, *TIMP-2* and *MT1-MMP* while *Endo180* was down-regulated. (C) Demonstration of MT1-MMP and Endo 180 expression in the odontoblast layer. Odontoblast nuclei were stained with DAPI (first and fourth panels). Sections were dual stained for MT1-MMP (green fluorescence) and Endo 180 (red fluorescence). MT1-MMP labelling was more intense in the odontoblastic layers from carious teeth (second panel). Yellow fluorescence represents coincidence of MTP1-MMP and Endo 180 (second panel). In contrast, Endo 180 labelling was more intense in the odontoblast layer from healthy teeth (third panel). Scale bar 30 μm. (D) Bar chart demonstrating relationship of gene expression profiles related to detection of infection, signal transduction and mineralization. Gene expression for TLR-4, TRAM, Mal/TIRAP, NF-κB, SMAD-2,-4, COL1A1 and COL1A2 were observed to be significantly up-regulated, while gene expression levels for TLR-2, MyD88 and IκBα were down-regulated in the odontoblast layer of carious teeth. Levels of mRNA were normalized against *ACTB*. All values depict means ± SD (n=6). *$P \leq 0.05$; ** $P \leq 0.02$.

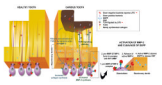

Figure 8.
Diagrammatic representation of the formation of reactionary dentin.

- Circular and uniformly distributed tubules are present in healthy teeth with odontoblast expression of TLR-2 but not TLR-4. DSP and MMP-2 are sparsely distributed.
- During extension of caries, LPS expressed by Gram negative bacteria triggers the TLR-4 signalling pathway which induces up-regulation of *MMP-2*, accompanied by up-regulation of *TIMP-2* and *MT1-MMP* (down-regulation of *Endo180* enhances MT1-MMP activity) resulting in cleavage of DSPP by activated MMP-2.
- DSP cleaved from DSPP is deposited on newly synthesised collagen forming nucleation sites for hydroxyapatite crystal formation.
- Low levels of TGF-β, released from dentin matrix and activated by bacterial acid or MMP-2, stimulate odontoblasts to increase collagen synthesis.